NASA Technical Memorandum 4272

Visualization Techniques to Experimentally Model Flow and Heat Transfer in Turbine and Aircraft Flow Passages

Louis M. Russell and Steven A. Hippensteele

JUNE 1991

NASA Technical Memorandum 4272

Visualization Techniques to Experimentally Model Flow and Heat Transfer in Turbine and Aircraft Flow Passages

Louis M. Russell and Steven A. Hippensteele
Lewis Research Center
Cleveland, Ohio

National Aeronautics and
Space Administration

Office of Management

Scientific and Technical
Information Program

1991

Visualization Techniques to Experimentally Model Flow and Heat Transfer in Turbine and Aircraft Passages

Louis M. Russell and Steven A. Hippensteele
National Aeronautics and Space Administration
Lewis Research Center
Cleveland, Ohio 44135

Summary

Increased attention to fuel economy and increased thrust requirements have increased the demand for higher aircraft gas turbine engine efficiency through the use of higher turbine inlet temperatures. These higher temperatures increase the importance of understanding the heat transfer patterns which occur throughout the turbine passages. It is often necessary to use a special coating or some form of cooling to maintain metal temperatures at a level which the metal can withstand for long periods of time. Effective cooling schemes can result in significant fuel savings through higher allowable turbine inlet temperatures and can increase engine life. Before proceeding with the development of any new turbine it is economically desirable to create both mathematical and experimental models to study and predict flow characteristics and temperature distributions. This report describes some of the methods used to physically model heat transfer patterns, cooling schemes, and other complex flow patterns associated with turbine and aircraft passages.

Introduction

In recent years rising fuel costs and increased thrust requirements have increased the demand for higher aircraft gas turbine engine efficiency. From basic thermodynamic theory, one of the more obvious ways to gain higher engine efficiency is to maximize the operating temperature. Higher temperature are easily obtained by adjusting the fuel to air ratio and altering the physical characteristics of the combustor. However, higher combustion gas temperature mean that the turbine will be exposed to higher temperatures which can cause thermal damage. Higher temperatures increase the importance of understanding the heat transfer patterns which occur throughout a turbine passage. It is often necessary to use a special coating or some form of cooling to maintain metal temperatures at a level which the metal can withstand for long periods of time. Effective cooling schemes can result in significant fuel savings through higher allowable turbine inlet temperatures. Effective cooling schemes can also increase engine life and reduce maintenance time. These savings have a direct impact on the cost of personal air travel as well as on the cost of products transported by air.

Before proceeding with the development of any new turbine it is economically desirable to create both mathematical and physical models to study and to predict flow characteristics and temperature distributions. Work has been done (ref. 1) and is continuing in the area of mathematical modeling. Reference 2 emphasizes the growing coordination between computational and experimental researchers in the area of heat transfer in aeropropulsion systems. The present report describes some of the methods used to experimentally model the heat transfer patterns which occur in the turbine region and the cooling schemes as well as other complex flow patterns associated with turbines. Experiments performed with these models are intended to answer such questions as: What is the expected location of areas of high heat transfer? Which blade or vane shapes are likely to produce hot spots on the surface? Where is internal or external cooling most needed? When does film cooling become excessive and how would this excessiveness affect heat transfer to the surface? Which cooling hole configurations are most effective under what conditions? To answer such questions experimentally, a small wind tunnel was used in conjunction with flow visualization and thermal visualization methods. Flow visualization and thermal visualization are vividly effective and inexpensive ways to study turbine flow phenomena and heat transfer.

The information contained in this report is a summary of flow visualization and heat transfer work performed by the authors over the past 15 years. This report was written primarily for those not necessarily working directly in these areas, but who have a technical or scientific background and a general interest in the subject matter. The report is based on a presentation made at the National Technical Association 57th Annual Conference, Houston, Texas, July 22–27, 1985. Those attending the conference had a wide variety of technical and scientific backgrounds. The information should also be useful to those working in the areas of turbine hardware design, turbine or engine heat transfer, and engine development. Some quantitative results were obtained which could be useful as computer code verification for those doing mathematical modeling of turbine flow and heat transfer. For more detailed information on any particular topic, the references listed can be consulted.

The Overall Engine

Figure 1 is a picture of a typical aircraft turbojet engine. Although this engine is made up of thousands of parts, the major components and their functions are as follows:

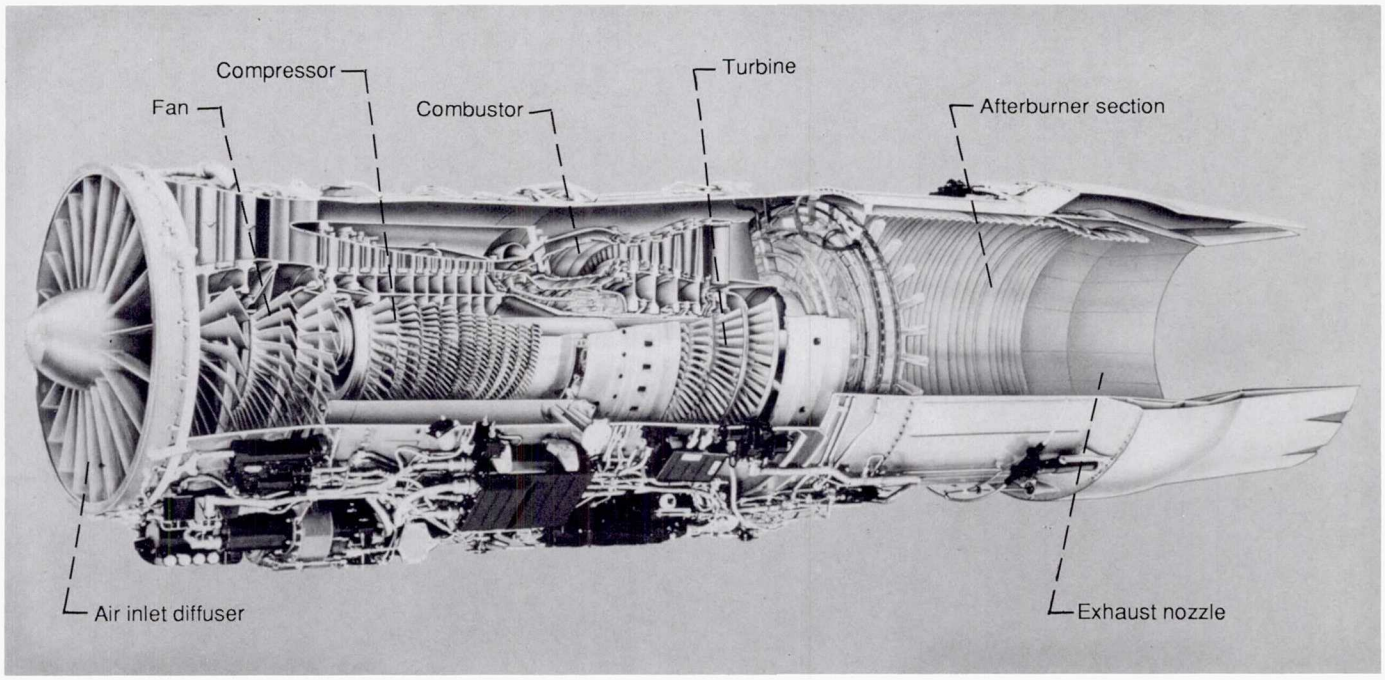

Figure 1.—Turbojet engine (F100-PW-100).

(1) The **air inlet diffuser** increases the static pressure of the incoming air by a factor of about three.

(2) The **fan** further increases the pressure and moves a large mass of air past the main air compressor.

(3) The **compressor** increases the pressure of the remainder of the air at a ratio of about 8:1.

(4) In the **combustor**, the fuel and air mixture is burned, producing large quantities of high pressure, high temperature gas.

(5) The **turbine** extracts some of the energy of the hot gases to drive the compressor and the fan. It also powers accessories such as the oil pump, fuel pump, and electric generators. The turbine in the engine shown is made up of four rows of stationary vanes and four rows of blades which rotate at about 14,000 revolutions per minute.

(6) The **afterburner** provides additional energy to the gas stream by the injection of raw fuel to react with any unburned oxygen in the gas stream.

(7) The **exhaust nozzle** accelerates the hot gases and expells them out the rear of the engine to produce thrust. The engine shown in figure 1 produces a maximum of about 106,750 newtons (24,000 lb) of thrust.

Although all these components are important in comprising the total engine, this report focuses on the turbine. Because of the very high rate of rotation, the turbine blades are exposed to great centifugal and bending forces. The blades and vanes are also exposed to very high temperature gases. The temperature of these gases generally varies between 1370 and 1650 °C (2500 and 3000 °F). These are higher temperatures than the metal surfaces can withstand without incurring heat damage. Since, as previously mentioned, the temperature of the combustion gases can be easily adjusted, it might seem that a readily available solution to the turbine heat problem would be to lower the combustion gas temperature. The reason this is undesirable is explained in the following discussion.

The amount of mechanical work which can be produced by a turbine is represented by

$$W = c_p \eta T_{in}[1 - (p_{ex}/p_{in})^{(\gamma-1)/\gamma}]$$

where

c_p heat capacity of the gas at constant pressure

η efficiency of the turbine

T_{in} turbine inlet gas temperature

p_{in} turbine inlet pressure

p_{ex} turbine exit pressure

γ ratio of heat capacity at constant pressure to heat capacity at constant volume

Although the turbine work can be affected by altering any of the variables, turbine inlet temperature is the one which is the most convenient to vary and, as the equation shows, turbine work is directly proportional to this temperature.

The amount of mechanical work which can be extracted from a turbine has a significant effect on the overall efficiency of an aircraft engine. A few percentage points of increase in engine efficiency can result in thousands of gallons of fuel being saved by a fleet of jetliners in a month's time. An

increase in overall engine efficiency can also increase performance (thrust) at the same rate of fuel consumption. This would be of major importance in military aviation.

The benefits of high turbine inlet temperature are lost, however, if these temperatures cause damage to the blade or vane surfaces. Such damage could mean, at best, a loss of turbine efficiency and, at worst, destruction of individual blades and vanes. When the high revolution rate of a turbine rotor (typically 14,000 rpm) is considered, it is not unreasonable to imagine a blade failure catastrophic enough to cause serious damage to the whole engine. Thus, high turbine inlet temperatures are desirable, but the turbine surfaces must be kept adequately cool.

Methods of Protecting Surfaces From High Temperatures

There are several methods of protecting the turbine surfaces from the hot gases. The following discussion outlines some of these methods.

Ceramic Thermal Barrier Coatings

Ceramic coatings are sometimes used to protect metal turbine surfaces from extremely high temperatures. A typical coating material is stabilized zirconia deposited onto a metal-to-ceramic bond coat of a nickel-chromium-aluminum-yttrium alloy. Stabilized zirconia is a useful coating material because it can withstand higher temperatures than can the underlying base metal. However, ceramic coatings tend to wear and/or spall after a period of time, exposing the bond coat and base metal to deleteriously high temperatures. It is difficult to predict when this will occur. In spite of these disadvantages, thermal barrier coatings are being successfully used to thermally protect base metals and to reduce base metal cooling requirements. Reference 3 summarizes the results of studies made on thermal barrier coatings.

Internal Cooling

Another method of protecting the surface is by extracting the heat using internal cooling. A fluid is passed through the internal passages of a blade or vane drawing heat away from the surface. A liquid such as water can be used but liquids, being relatively heavy, would impose a large weight penalty, particularly for long duration flights. Since air is a fluid that does not impose a weight penalty, it is used almost exclusively for cooling aircraft turbines. A convenient source of this air is the compressor. A small quantity of air is extracted from the compressor and is used to cool the turbine. Although this air is typically between 350 and 450 °C (660 and 840 °F), it is relatively cool compared to the 1370 to 1650 °C (2500 to 3000 °F) temperatures of the hot gases to which the turbines are exposed.

Figure 2 is a cutaway view of a cooled turbine vane. It shows a few types of both internal and external cooling methods. Near the leading edge, convection cooling is used. Air is passed through the corrugated passages. This helps to cool the leading edge of the vane which experiences some of the highest heat loads. Near the trailing edge, fins (in the form of posts) are used to produce turbulence which leads to increased heat transfer to the cooling air. In the middle region, impingement cooling is shown. Tiny streams of air are forced through the holes to impinge on the inner surface of the outer skin. Again the high turbulence results in increased heat transfer to the cooling air. The heated air from these forms of internal cooling may be discarded through slots at the trailing edge.

External Cooling

Air may also be discharged over the vane exterior surface as in external film cooling. A single row of discrete film cooling holes is shown in figure 2. Multiple rows may also be used. The thin film of relatively cool air discharged over the surface acts as a buffer between the hot gases and the surface, maintaining the surface temperatures considerably lower than the hot gas temperature. Film air may also be injected through slots as shown near the trailing edge in figure 2. A method not shown in the figure is transpiration cooling where the outer skin is made of a porous material. Cooling is accomplished by air effusing through the skin as well as by the thin film which then forms on the surface. Of the three external cooling methods, the discrete hole arrangement is the one most commonly used. Its advantage over the slot method is its lower fabricating cost and over the transpiration method is its better structural integrity.

All these methods of providing cooling use a small amount of air from the compressor and cause increased manufacturing costs; however, the gains in fuel economy and decreased maintenance costs resulting from effective cooling schemes usually offset the increased manufacturing costs. Cooling, however, should not be done arbitrarily. Poor external cooling schemes can actually result in higher surface temperatures than would have occurred without cooling. They can also result in intolerable aerodynamic losses if there is excessive interference with the mainstream. The flow fields around turbine passages are quite complex. This can be seen in figure 3 which shows typical flow patterns around a rotating turbine blade. The addition of external cooling further complicates the flow, and these flow patterns can have a profound effect on the heat transferred to the surface from the hot gases. External cooling must be done in a manner which produces a minimum of disturbance to the mainstream and the boundary layer, a thin film of relatively low velocity fluid which occurs when any fluid passes over a surface. This boundary layer alone provides a partial barrier between the hot gases and the surface. Effective external cooling such as film cooling enhances this protection.

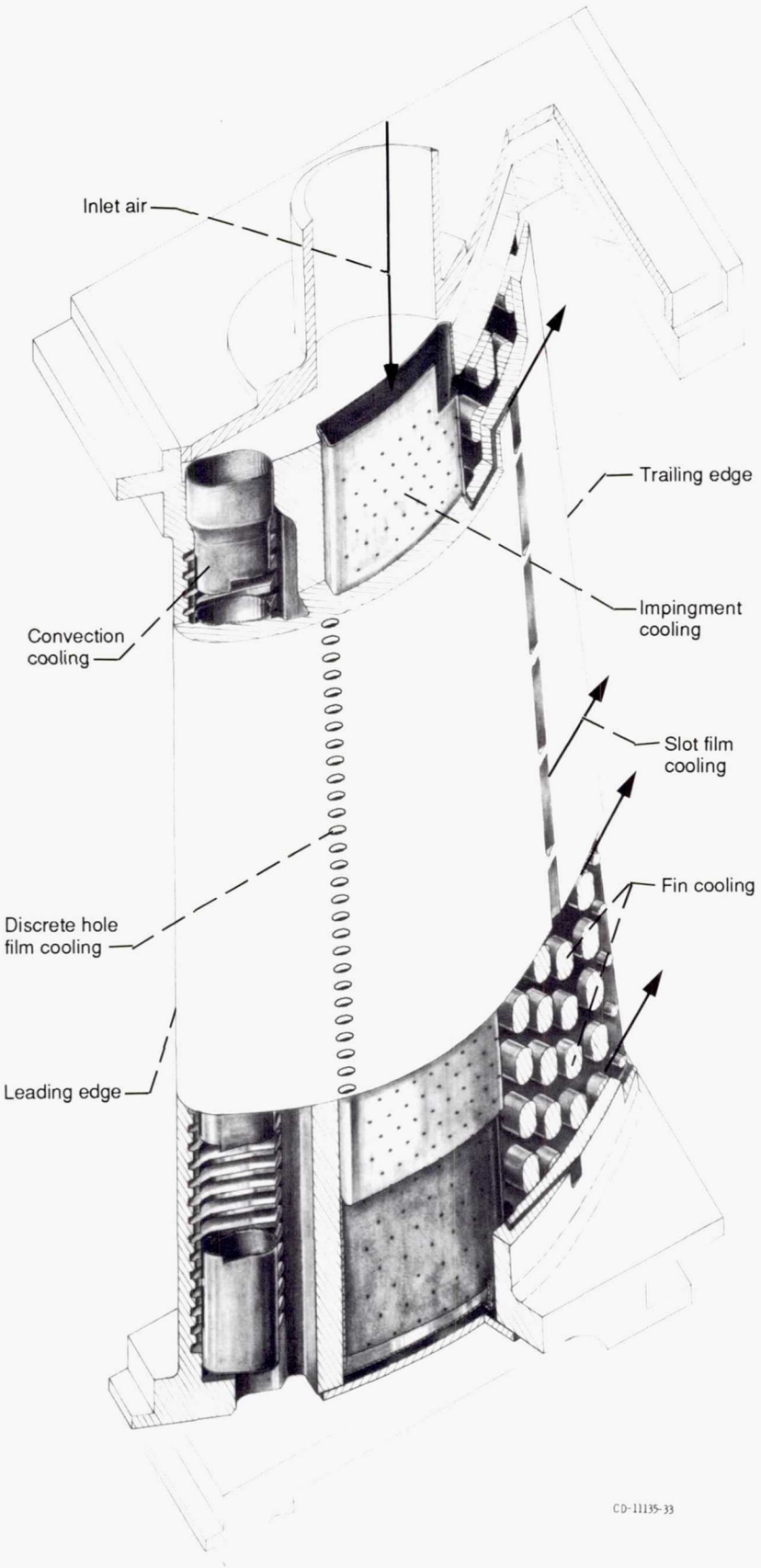

Figure 2.—Cooled turbine vane.

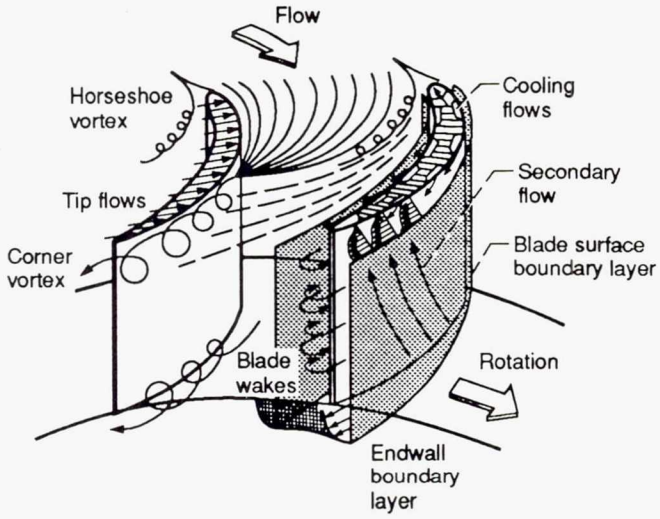

Figure 3.—Turbine blade external flow patterns.

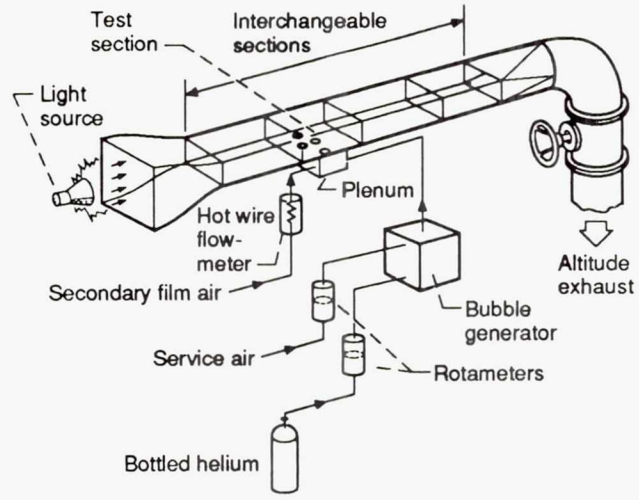

Figure 4.—Flow visualization test facility.

Test Facilities

The tests were performed in two facilities. One was a wind tunnel using ambient temperature air and the other was a water tunnel using tap water seeded with tiny magnesium oxide particles.

Air Tunnel Facility

Figure 4 is a picture of the wind tunnel used for most of the tests. Ambient temperature air was drawn through the tunnel into a vacuum exhaust system. A maximum of 8.2 kg/sec (18 lb/sec) of air could be drawn through the tunnel. Most of the tunnel including the test section was made of clear plastic. The test section could vary widely depending on the configuration being simulated. For example, when flow in a turbine passage was being simulated, the test section was a blade or vane cascade. (A cascade is a row of blades or vanes situated to simulate the flow which would be experienced in a real turbine. A vane cascade will be shown on a later figure.) In figure 4, film cooling of a flat plate was being simulated, so a straight test section with a flat floor was used.

Water Tunnel Facility

Figure 5 is a schematic diagram of the facility used for the digital imaging experiments. It consisted mainly of a water tunnel capable of flowing up to 65 gallons of water per minute, a 2-watt laser system, a video recording system, and a personal computer with digitizer. The water passed from a supply tank to a receiver tank through a clear plastic test section. As with the wind tunnel, the test section could vary depending on the configuration being tested.

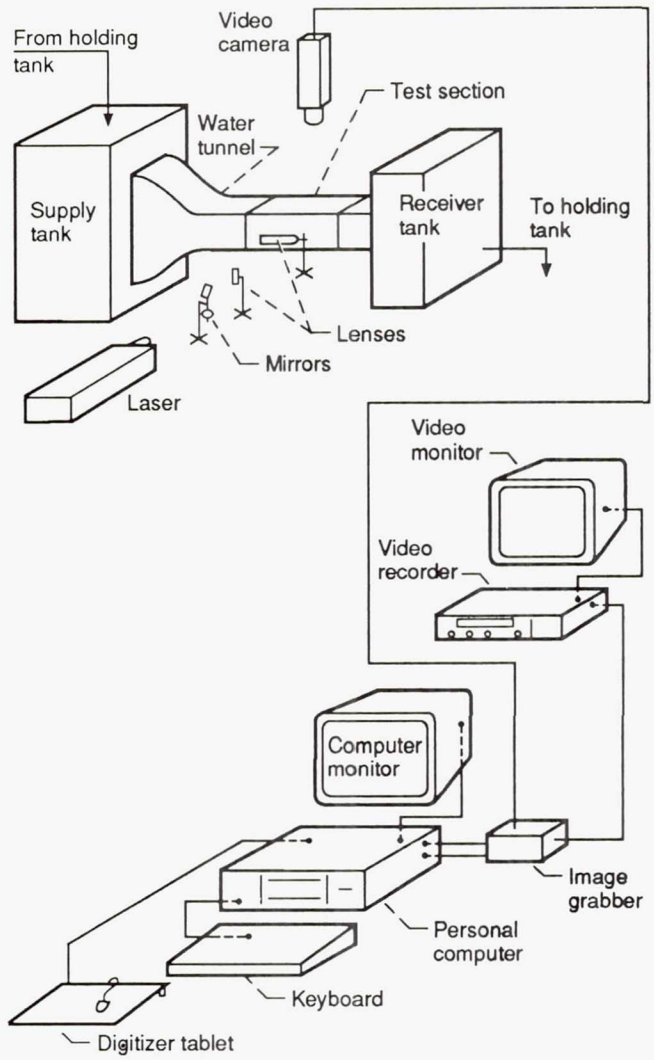

Figure 5.—Fluid flow digital imaging schematic.

Experimental Techniques and Applications to Studies of Turbine and Engine Passages

Bubble Streakline Flow Visualization

Two examples will be given to illustrate the type of information obtained using bubbles to visualize flow. One is a simulation of film cooling of a flat surface. Figure 6 is a closeup view of the straight, flat plate test section which contained an array of four film cooling holes. Air was introduced into a plenum below the test surface along with the bubbles which were produced by a commercially made bubble generator. The helium-filled soap bubbles were about 1 mm in diameter and were neutrally buoyant in air. (More details of this bubble generator system are available in ref. 4.) The plenum air seeded with bubbles was injected into the mainstream through the simulated film cooling holes. The bubbles in the injected stream were illuminated by a high intensity lamp. When photographed, the results were streaklines which mapped the flow field. Mainstream velocity was measured by the total pressure probe shown just upstream of the test section. The surface boundary layer was also surveyed at this location.

Figure 7 shows the top and side views of the streakline patterns resulting from photographing the injection of a stream of bubbles and air over a flat surface into the mainstream. Two different hole configurations were compared—inline and compound angle. With inline injection, the holes were angled 30° from the surface and pointed in the direction of the mainstream. With compound angle injection, the holes were also angled 30° from the surface but pointed in a direction 45° from the mainstream. The *blowing ratio m* was high in both cases, about 0.75. (Blowing ratio $m = \rho_{inj}V_{inj}/\rho_{fs}V_{fs}$ where $\rho_{inj}V_{inj}$ is the density times velocity of the injected film and $\rho_{fs}V_{fs}$ is the density times velocity of the free stream.) The boundary layer thickness is indicated on the side view. Comparing the side views in figure 7 shows that the main bulk of the injected stream is closer to the surface with compound angle injection, which in a real engine would provide better thermal protection. The slight void seen below the in-line stream would allow hot gases to move below the film and contact the surface. Lateral coverage is also slightly better with compound angle injection. This illustrates that when high blowing ratios are necessary angling the holes in a compound manner would be advantageous. More comparisons among other film cooling configurations are given in detail in reference 5.

Another illustration of the use of helium bubbles for flow visualization is the modeling of the so-called *horseshoe vortex*. This is a particularly harmful vortex in terms of its effect on heat transfer to the surface. It begins in front of the leading edge of a blade or vane near the flat endwall surfaces. It separates into two legs, one around each side of a blade or vane. This flow was visualized using the two-dimensional vane cascade shown in figure 8. Figure 9 shows a typical result.

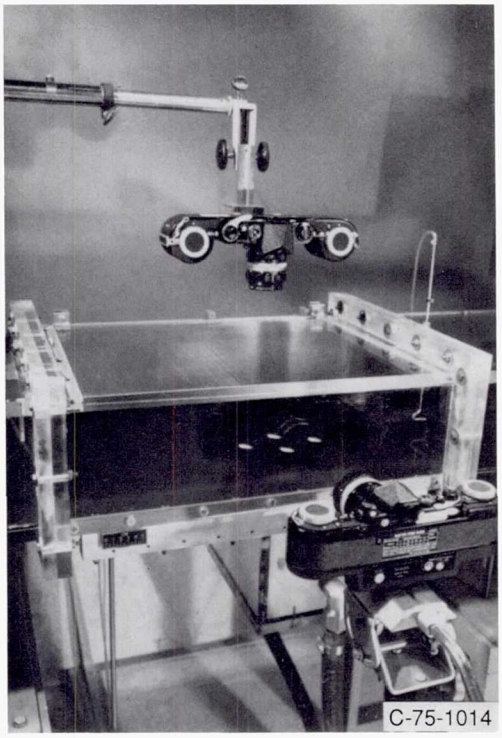

Figure 6.—Flat-plate film-cooling test section.

It is a view looking vertically down at the endwall. All the bubbles were not illuminated for this photograph. Using a thin sheet of light illuminated only those bubbles close to the flat surface where the vortex occurs. The corkscrew-like path of the flow can be seen as two of the bubbles are caught in the vortex. In a real engine the high turbulence associated with this vortex increases the heat transfer from the hot gases to the surface. This type of information illustrates, for a particular design, the existence of the horseshoe vortex, its strength, and its location so that steps may be taken to reduce its harmful effect. A more detailed discussion on the visualization of the horseshoe vortex can be found in reference 6.

Smoke Flow Visualization

Even though the bubbles are small in diameter, they are sometimes large relative to the flow field being studied—for example, a thin boundary layer on the leading edge of a turbine vane. In such instances, a smoke generating apparatus was used in place of the bubble generator shown in figure 4. In this study, the *smoke* was actually a cloud consisting of carbon dioxide gas and mineral oil. This device, like the bubble generator, was also commercially acquired. The test section shown in figure 10 illustrates the use of smoke in visualizing film injection over a cylinder in crossflow. The smoke-air mixture, which simulated film cooling air, was injected through the two tubes shown. The tubes could be installed at

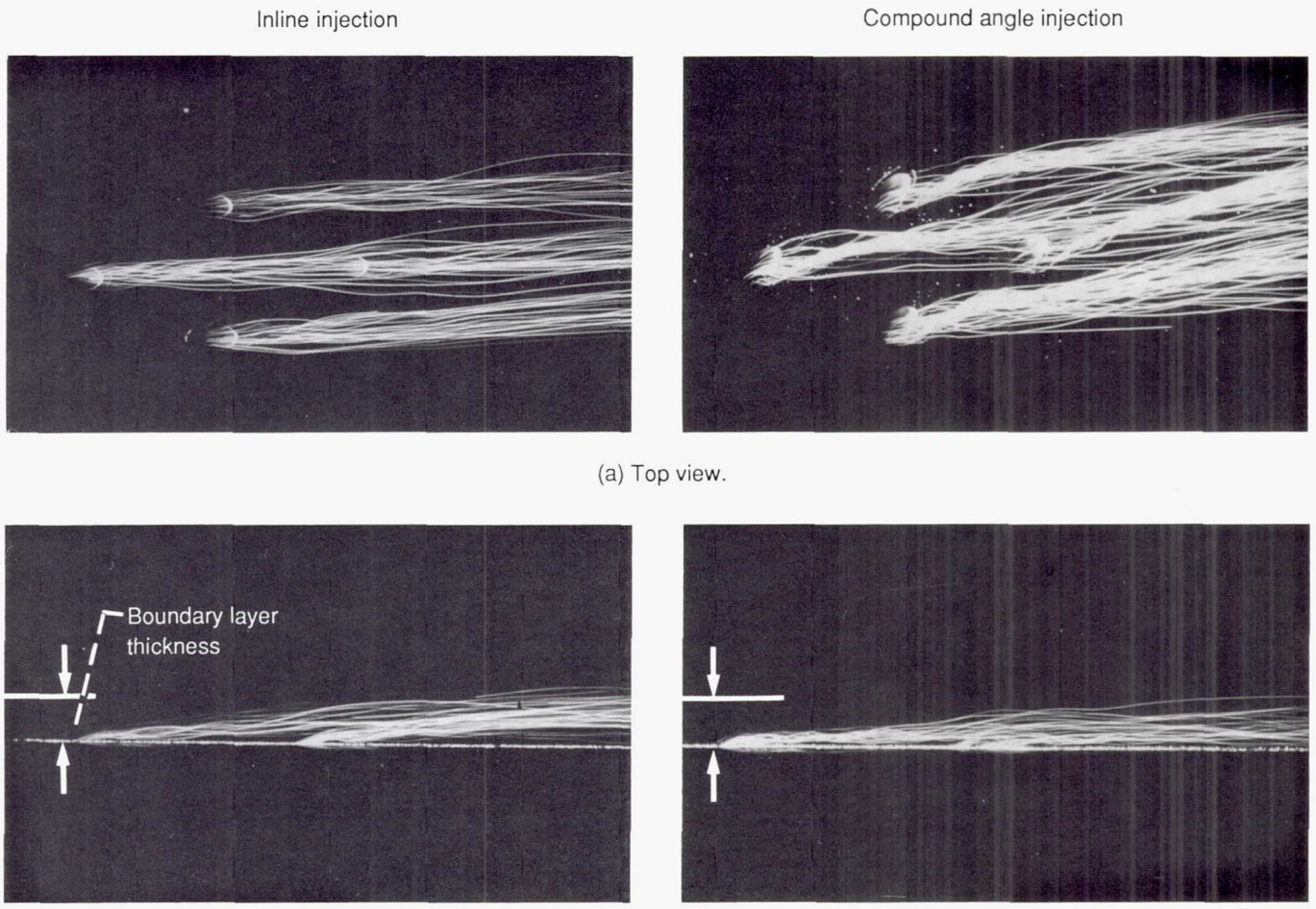

(a) Top view.

(b) Side view.

Figure 7.—Bubble streakline flow visualization of film cooling.

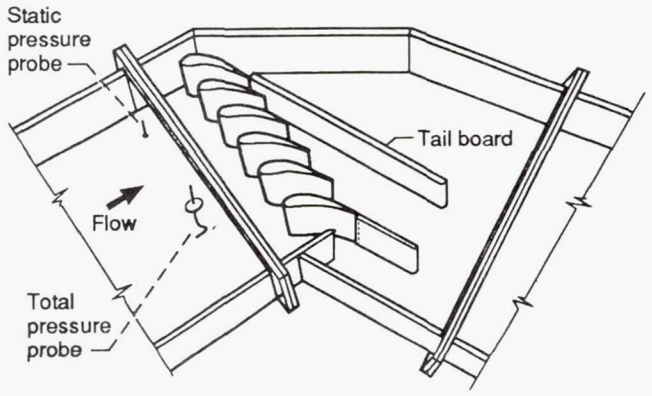

Figure 8.—Vane cascade test section.

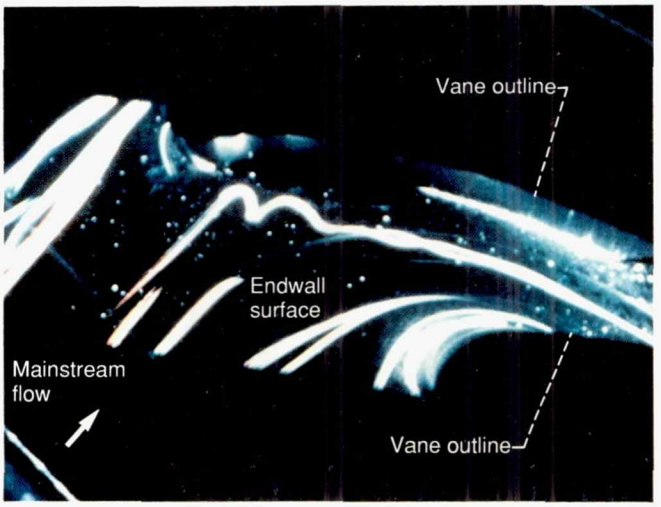

Figure 9.—Bubble streakline flow visualization of a horseshoe vortex.

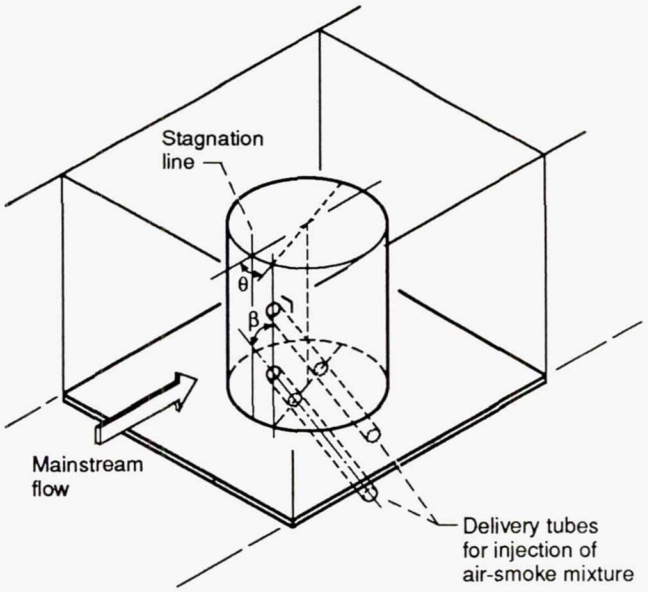

Figure 10.—Leading-edge cylinder test section.

various angles β from the surface, and the cylinder could be rotated at various angles θ relative to the mainstream. Another variable was the blowing ratio m (previously defined). This configuration roughly simulated film cooling of the leading edge of a turbine vane. The smoke plume, when illuminated, shows the general path of a mass of air, but it is not as effective as the bubbles in revealing the detailed particle paths in turbulent flow fields.

Figure 11 shows a typical result. This is a view looking vertically downward on the cylinder. The injection angle β was 30° from the surface, and the injection location θ was 60° from the stagnation line. (The stagnation line represents that location on the leading edge of a blunt body where the flow velocity is zero.) The figure illustrates that in a real engine at injection locations away from the stagnation line (stagnation

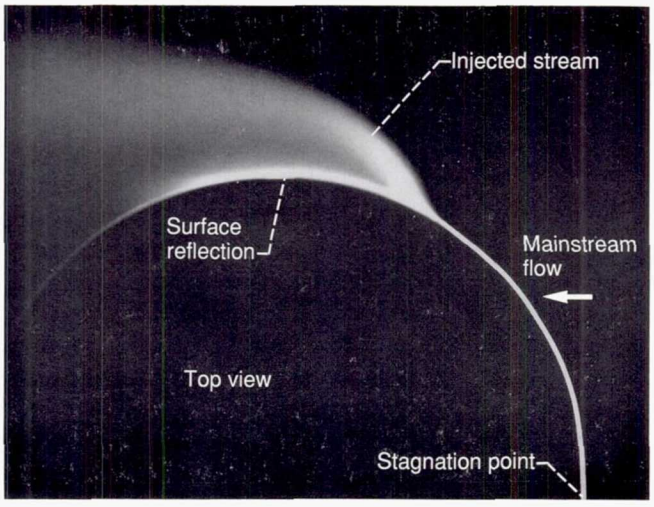

Figure 11.—Smoke flow visualization of leading-edge film cooling.

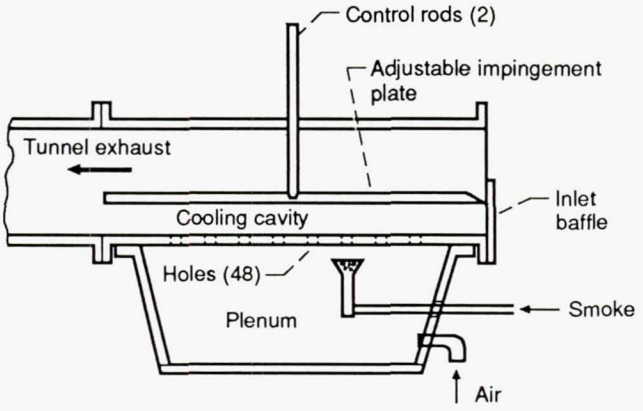

Figure 12.—Smoke flow visualization of impingement cooling. Material, clear acrylic.

point in a top view), the *protective film* does not lie close to the surface but separates from the surface, providing practically no film protection from the hot gases. A full discussion of the results at various combinations of blowing ratio, injection angle, and angular distance from the stagnation line is given in reference 7.

Another test section in which smoke flow visualization was used is shown in figure 12. This test section simulated impingement cooling, one of the methods of internal cooling previously mentioned. In this situation there were no tunnel sections upstream of the test section. Generally the mixture of smoke and air was injected into the plenum. The mixture, under slight pressure, flowed through holes in the plenum plate and impinged on the impingement plate. For some of the tests it was necessary to aim a stream of smoke directly at a specific hole to get the desired visual effects.

One question of interest was whether an impingement jet stream behaves more like a solid cylinder (pin fin) when subjected to a crossflow or whether it is swept along by the crossflow. Another question involved physical arrangement of the impingement holes. Heat transfer studies have indicated that an inline hole arrangement provides more effective cooling than a staggered hole arrangement (ref. 8). Smoke flow visualization was used in an attempt to reveal the reason for this.

The answer to the question about the jet stream can be seen in figure 13, which is a top view and a side view of a smoke impregnated jet (on the right) impinging on a transparent plate. The jets of air from the two downstream holes seem relatively undisturbed by the crossflow. Thus, the jets remain relatively intact to impinge on the surface while forcing the upstream air to flow around them. The answer to why the inline hole arrangement provides more effective internal cooling than the staggered arrangement could be seen visually using smoke. With the inline arrangement, the closer proximity of each hole to its downstream neighboring hole creates greater overall turbulence than with the staggered arrangement. In a real turbine this would result in greater heat transfer to the coolant air.

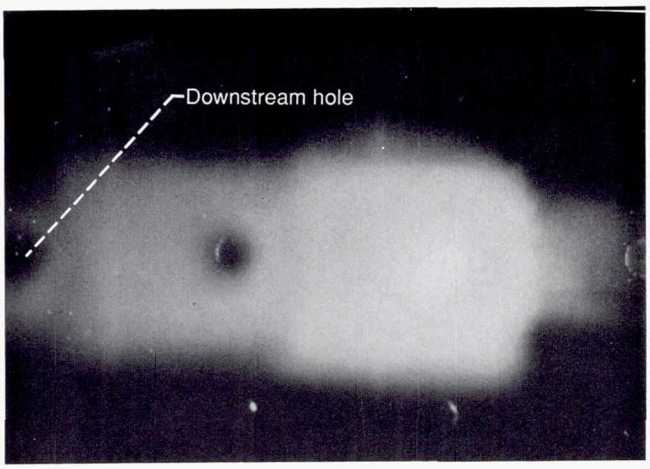

(a) Top view looking through impingement plate.

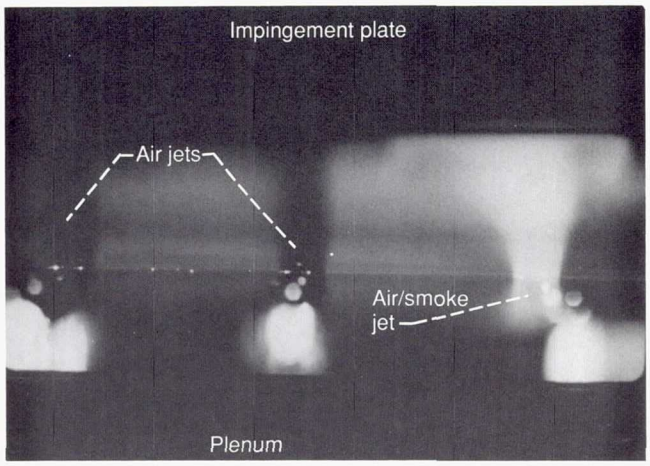

(b) Side view of cooling cavity.

Figure 13.—Smoke flow visualization of impingement cooling – inline pattern.

Ink Dot Surface Flow Visualization

In addition to internal flow and external flow in turbine passages, it is also advantageous to study the flow directly at the surface. Methods in which a material is deposited on the surface and reacts to the surface shear stress are popular. One such method is the ink dot technique originated at the University of Connecticut (ref. 9). Ink dots were placed on the surface at strategic locations before tunnel flow was initiated. The dots were flooded with oil of wintergreen which partially dissolved the ink, and then tunnel flow was established. The dissolved ink dots responding to the shear forces traced the path of the air at the surface.

Figure 14 shows a typical result of the ink dot method. This view is looking vertically downward on a row of vanes after air had been drawn through the test section. The path of the dissolved ink traced the streamlines of the flow on the end wall surface. One pattern that can be observed within the

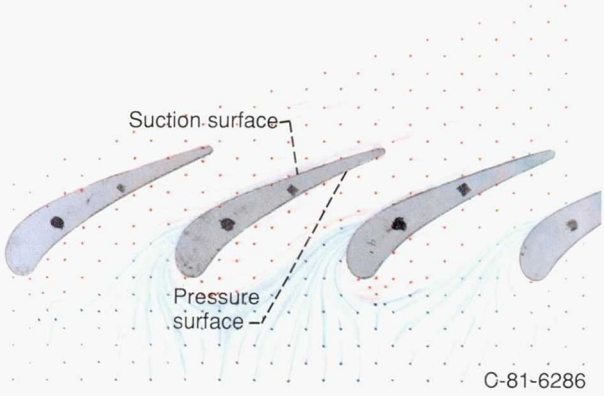

Figure 14.—Ink dot surface flow visualization.

passage between the vanes is the drifting over of the flow from the pressure (concave) side of one vane to the suction (convex) side of the adjacent vane. This corresponds to the general path taken by one leg of the horseshoe vortex previously discussed. Two different regions of flow on the endwall are illustrated by the different colors. Near the surface, much of the inlet flow, represented by the blue traces, is channeled sharply toward the front of the suction side of each vane. In a real engine this would cause warmer gas to come closer to other parts of the surface, as represented by the red traces.

Oil Smear Surface Flow Visualization

Another method of studying flow at a surface was also used. Mineral oil mixed with yellow pigment was smeared on the test surface before tunnel flow was initiated. Flow was then established. Any anomalies such as flow separations were revealed in the form of either discontinuities or accumulations in the oil patterns.

The results of the oil smear method of studying surface flow visualization are illustrated in figure 15. This is a view looking obliquely downward at the pressure (concave) side of a test blade which had been smeared with yellow pigmented mineral oil before flow was initiated. In the *after flow* portion of the picture, the accumulation of oil just downstream of the leading edge is the result of a separation of the flow from the surface, a flow anomaly. The void region just downstream is where the flow reattached strongly to the surface, pressing away the oil at this point. In a real engine the separated region would be a relatively cool spot and the reattachment region would be a very hot spot as the gases come back in contact with the surface. Such temperature gradients over a small area would result in severe thermal stresses in the surface material with their associated potential for damage.

Digital Imaging of Fluid Flow

The digital imaging experiments were performed in a cooperative agreement between NASA and The University of

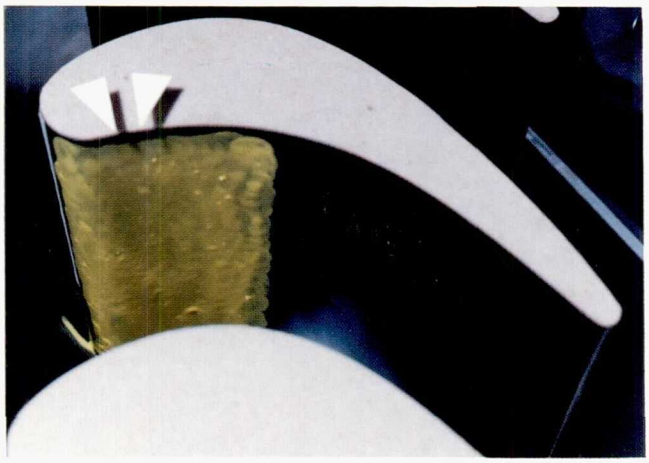

(a) Before airflow started, pressure side.

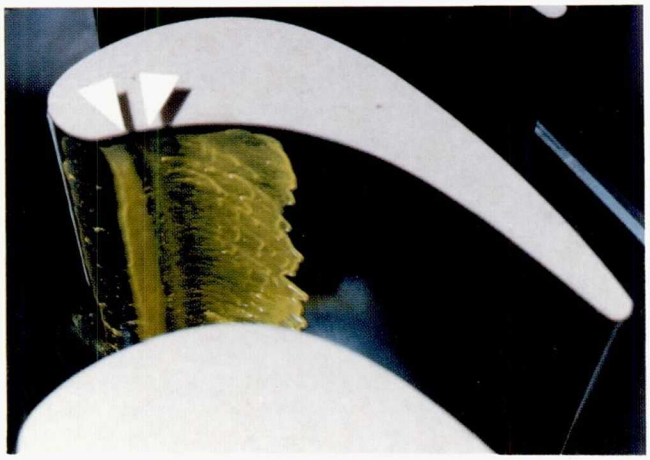

(a) After 2 minutes of airflow, pressure side.

Figure 15.—Oil smear surface flow visualization.

Akron using the water tunnel referred to in figure 5. The water was seeded with tiny magnesium oxide particles and the flow field under study was illuminatd by a thin sheet of laser light. A video camera was used to obtain magnified images of a slice of the flow field. These images were digitized, stored on magnetic disks, and then computer processed into quantitative data in the form of positions, directions, velocities, and accelerations. An example of the use of this method is shown in figure 16. Figure 16(a) represents an aircraft engine inlet cowl lip. The hypersonic velocities expected in the next generation of aircraft will produce very high temperatures on the external surface simply from aerodynamic heating. It will sometimes be necessary to use some internal cooling to help remove some of this heat. The test section used in this study, shown in figure 16(b), roughly simulates this situation. Video images were obtained of the flow patterns which occur in the internal passage. A typical example is shown in figure 16(c), which is a single frame taken from the video tape. These patterns can have a strong affect on the temperature distribution within the passage of a real engine. A typical end product of these experiments is shown in figure 16(d). It represents trajectories and velocities at selected locations in the flow field. Accelerations could also be shown. The quantitative results of these tests offer strong potential for use in validating analytical computer codes of fluid flow. For more details about this method and the results see reference 10.

Liquid Crystal Thermal Visualization

Temperature patterns.—A method has been developed for studying temperature patterns and obtaining heat transfer coefficients on simulated turbine surfaces. In this method a composite sheet is made, consisting of some conductor material such as carbon impregnated paper, metal foil, or vapor deposited gold, laid back to back with a sheet of liquid crystal material. The composite sheet was attached by adhesive to the surface under study. The type of liquid crystals used has the property of changing color with temperature. The blue color corresponded to the highest temperatures with green, yellow, reddish brown, and black corresponding to decreasing levels of temperature. Since the yellow color occurred over the narrowest temperature band (about 0.06 °C (0.11 °F)), it was used as the calibrated surface temperature T_s. In this study, temperature was controlled by introducing an electric current through copper bus bars attached to the conductor sheet. The liquid crystal was precalibrated so that the color-temperature relationship was established. The composite sheet was attached to the surface of interest, electric heat was applied, air flow was established, and temperature patterns were recorded photographically. Figure 17 shows the test section used to study impingement cooling. This test section is the same one that was shown in figure 12 for smoke visualization of impingement cooling, but it was inverted in order to give a downward view of the liquid crystal surface. The composite sheet, attached to the test surface, was heated by the electric power supply until the calibration temperature was exceeded. Air was introduced in the form of impingement jets through holes in the plenum plate. The resultant color-temperature patterns (isotherms) on the liquid crystal sheet were observed and photographed. This use of the liquid crystal method to study temperature patterns is discussed more thoroughly in reference 11 along with more details about liquid crystals.

Figure 18 shows the temperature patterns resulting from the two different impingement cooling hole arrangements (inline and staggered) discussed in the smoke visualization tests. The view is looking downward through the transparent plenum, through the perforated plate, and onto the liquid crystal/heater composite. The composite sheet lies on a surface which simulates the inner surface of the outer skin of a turbine vane. It should be kept in mind that impingement cooling is one of the internal cooling methods where high heat transfer rates are desirable in order to pull heat away from a surface. This is opposed to external cooling where low heat transfer rates between the hot gas and the surface are sought. In figure 18

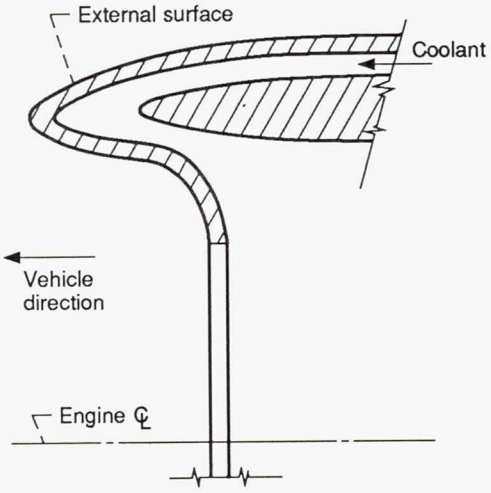

(a) Aircraft engine inlet cowl lip.

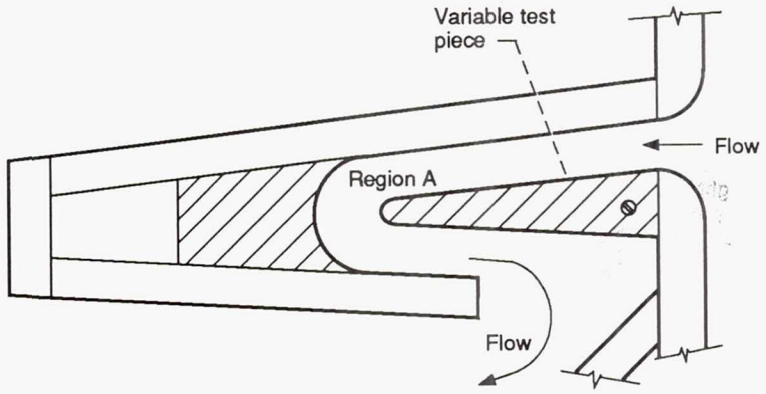

(b) Cowl lip test configuration.

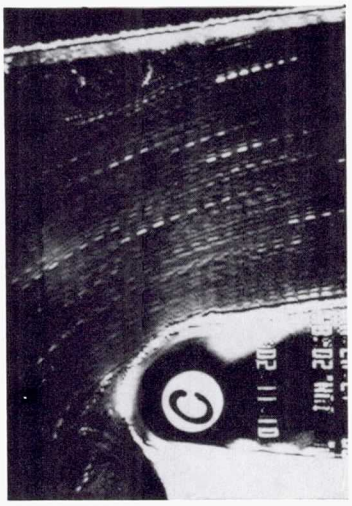

(c) Video image of flow field.

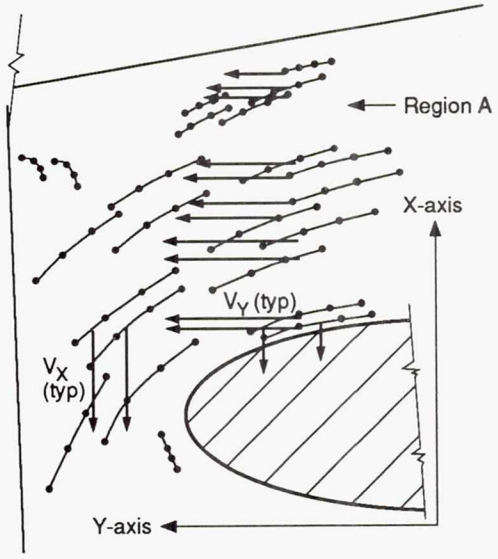

(d) Quantified flow trajectories and velocities.

Figure 16.—Digital imaging of fluid flow.

the relative cooling effectiveness of the two arrays is indicated by the relative extent of the dark (cool) areas inside the yellow isotherms. Comparison of the two arrays shows that for the same condition of flow the in-line hole array has larger areas of high heat transfer and is therefore more effectively cooled than the staggered hole configuration. This result is consistent with those found by Metzger and Florschuetz (ref. 8). Other applications of the liquid crystal method for studying temperature patterns are given in reference 11.

Flow anomalies.—The liquid crystal method can be used to study flow anomalies on simulated turbine surfaces. In this study, information was gained about the suspected flow separation bubble indicated by the pigmented oil method. Figure 19(a) is a view looking obliquely down at the pressure (concave) surface of a test blade during a test run. Evidence of the flow separation bubble just downstream of the leading edge is visible. Since the freestream air is at room temperature and the test surface is heated, the dark blue (hot) region just behind the leading edge is an area of low heat transfer, indicating that the flow had stagnated in this area. This is where the bubble is presumed to have formed. The black (cool) area just downstream of this region is an area of high heat transfer between the freestream and the surface, probably because of the air reattaching to the surface after it passed over the bubble. Of course, in a real engine with its hot freestream this would be a hot area. The location of the separation bubble and reattachment evidenced by this method corresponds with the location previously shown using the oil smear method on the same blade. More details of these results are given in reference 12.

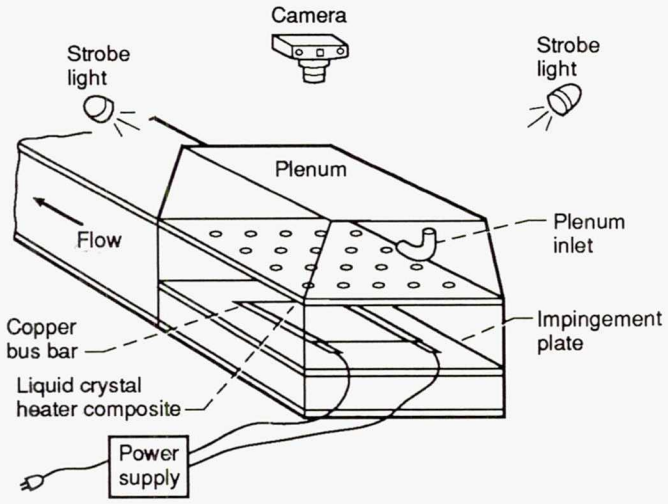

Figure 17.—Thermal visualization of impingement cooling.

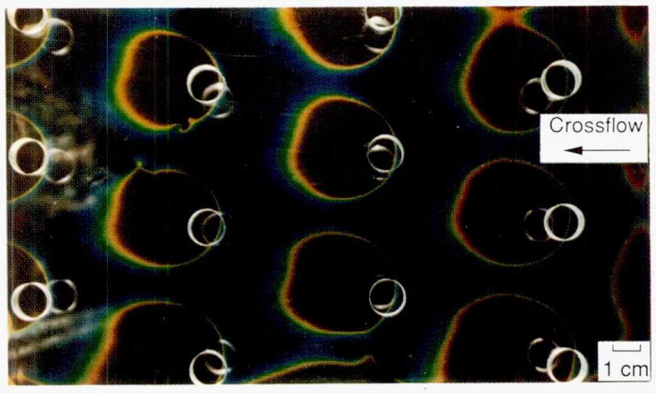

(a) Staggered array.

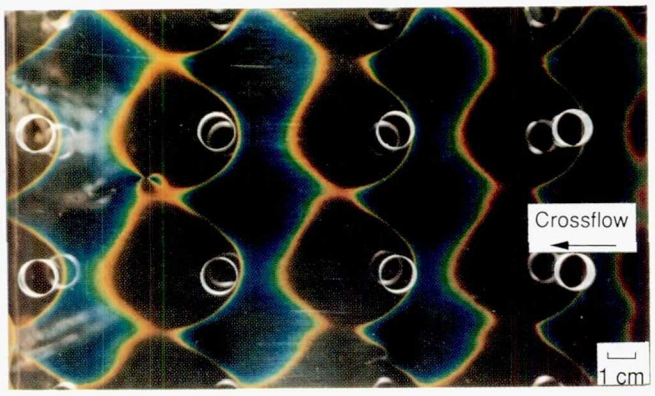

(b) In-line array.

Figure 18.—Thermal visualization of impingement cooling.

Liquid Crystal Quantitative Heat Transfer Measurements

Steady-state method.—One of the major objectives of the liquid crystal project was to obtain quantitative heat transfer results. This was done using the five blade cascade test section that had been used both with the oil smear and with liquid crystals to observe the effects of the flow separation bubble. The liquid crystal/heater composite sheet was wrapped completely around and attached to the test blade airfoil surface. The test blade was located at the center position of the row of blades. The liquid crystal sheet attached to the blade had been previously calibrated for color-temperature correspondence. Photographic data were taken during tunnel flow after steady-state conditions were reached. Heat transfer coefficients h were calculated as a function of surface distance using the heat balance equation

$$Q = hA(T_s - T_a)$$

where Q is the measured electrical heat input, T_a the measured freestream air temperature, T_s the surface temperature (indicated by yellow color), and A the measured heated area.

Values were obtained at three mainstream velocities: 67, 36, and 24 m/sec (220, 118, and 79 ft/sec). These coefficients are presented in figure 19(b). As the figure shows, the heat transfer coefficient near the leading edge was very high but dropped to a minimum in the pressure surface separation bubble region. Downstream of the separation bubble the coefficient reached a peak as the flow reattached to the surface. On the suction (convex) surface, the heat transfer coefficient was very high near the leading edge, decreased with surface distance to a minimum, and then increased rapidly near the trailing edge.

Another way that quantitative data can be reported is seen in figure 20. In this case the liquid crystal/heater composite was attached to the end wall surface between vanes instead of on the airfoil surface. Figures 20(a), (b), and (c) show the temperature pattern on the end wall during a test run at three levels of electrical power input and at constant freestream velocity. Figure 20(d) shows the resulting constant heat transfer lines calculated using these temperatures. Plots of this type and the one shown in figure 19(b) are very useful for quick identification of areas of high heat transfer along with quantitative values of the heat transfer coefficient. A more detailed discussion of the use of liquid crystals to study heat transfer on the turbine end wall is given in reference 13.

Transient method using spray-on liquid crystals.—In addition to the sheet material, liquid crystals may also be sprayed onto a test surface. This is necessary when the test surface is not a simple two-dimensional shape but a compound curvature shape such as a hemisphere. The spray-on method allows further options. Very fast responding liquid crystal solutions can be mixed to produce more than one calibration temperature on the same surface. This allows the transient temperature technique to be applied whereby, instead of using a layer of conductor as a heater, the whole test model is heated above the highest calibration temperature and the surface is allowed to cool through the lower calibration temperature while room temperature air is drawn over the surface during

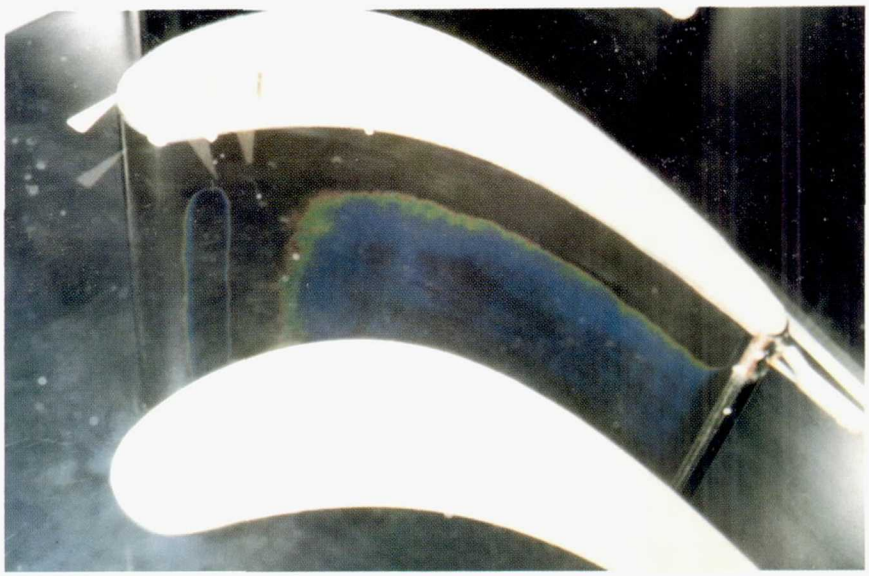

(a) Thermal visualization of airfoil surface.

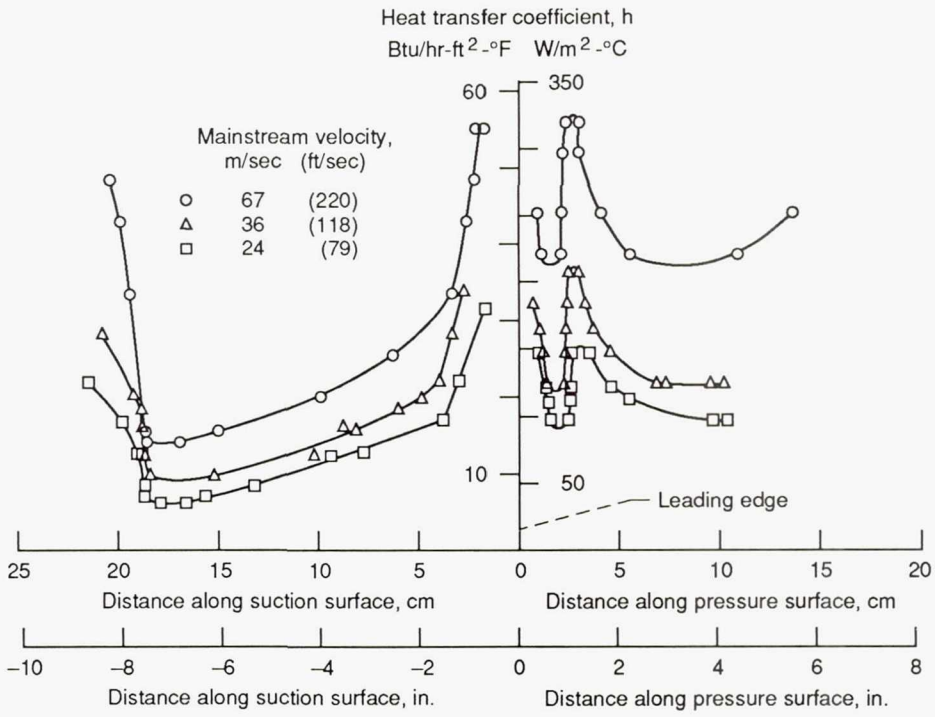

(b) Heat transfer coefficient map.

Figure 19.—Liquid crystal blade heat transfer.

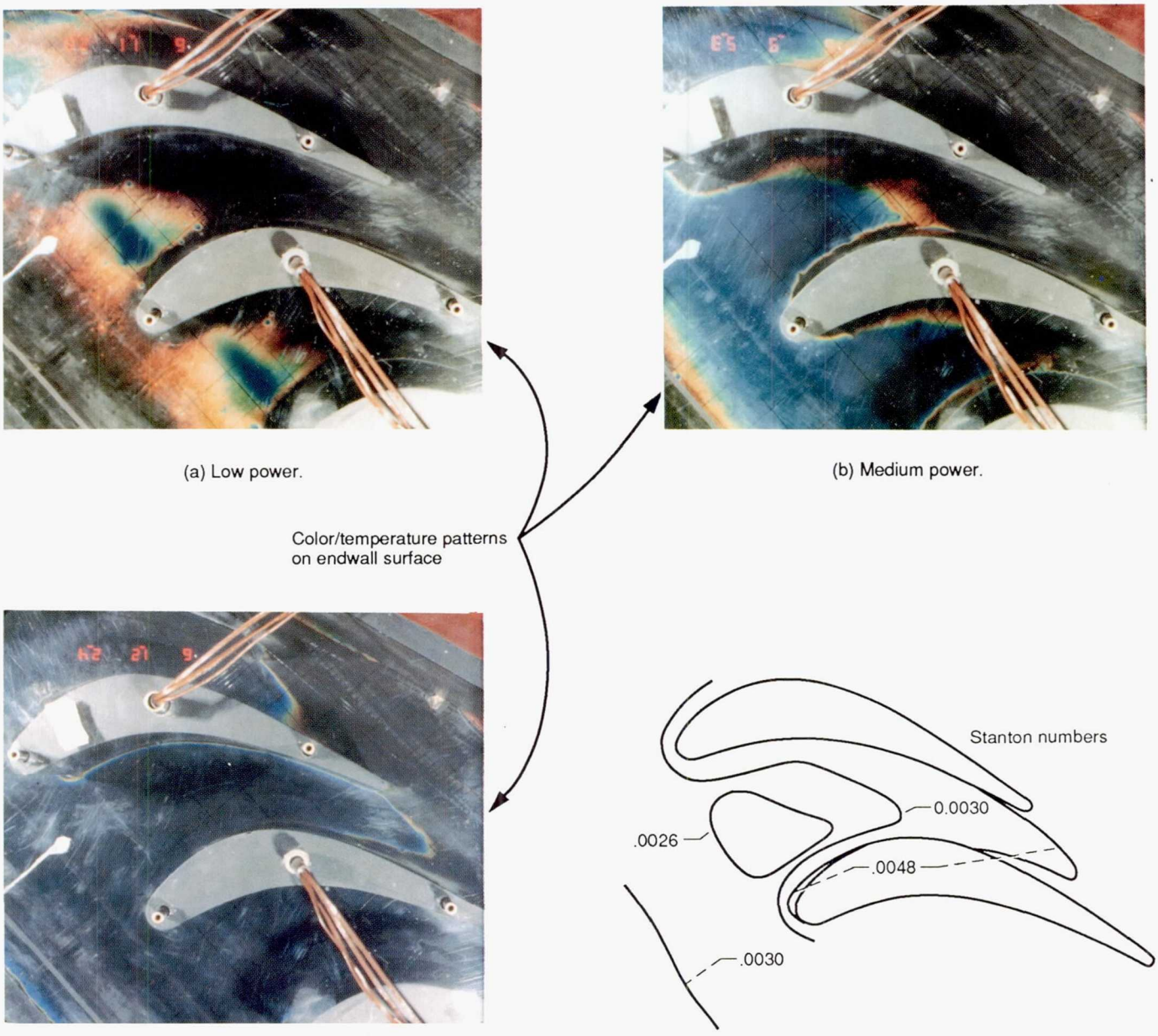

Figure 20.—Liquid crystal sheets for measurement of turbine endwall heat transfer. Reynolds number, 284 000. Yellow isotherm location varies with applied electrical power to map heat transfer contours.

a test run. The temperature T data along with the elapsed time t enables a calculation of heat transfer coefficients using the thermal diffusion equation

$$\frac{\partial^2 T}{\partial y^2} = \frac{1}{\alpha}\frac{\partial T}{\partial t}$$

and the heat flux at the surface

$$Q = h(T_a - T_s) = -k\frac{\partial T}{\partial y}$$

In these equations, α is the thermal diffusivity of the model wall, k is the thermal conductivity of the wall, and y is the distance into the wall. For details on the solution of these equations and a more thorough description of this method, see reference 14.

(a) Higher temperature liquid crystal, early in test run.

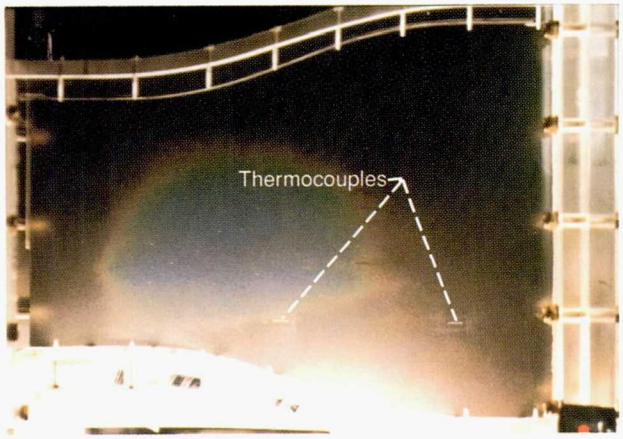

(b) Lower temperature liquid crystal, late in test run.

Figure 21.—Photographs of transient liquid crystal patterns on duct floor.

Typical results of the transient heat transfer method are shown in figure 21. This is a view looking vertically downward on the floor of a transition duct test section. Transition is from one duct shape to another at a constant cross sectional area. A dual temperature liquid crystal mixture was used. The figure shows the color patterns at the two temperature levels at different times during the run. Thermocouples were used at two locations to verify the liquid crystal temperatures. Figure 22 shows yellow color positions as a function of time after room temperature air was allowed to flow through the test section.

The advantage of the liquid crystal method over conventional experimental heat transfer methods was demonstrated by the liquid crystal method's ability to give continuous, quantitative, high-resolution heat transfer information at any desired location on the test surface. A limitation of the method is the temperature tolerance of the liquid crystals. The maximum temperature at which experiments can be performed is about 93 °C (200 °F).

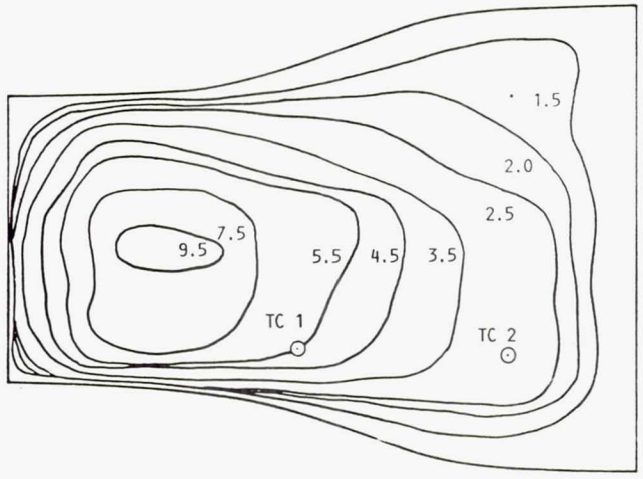

(a) Higher temperature liquid crystal (yellow = 42.4 °C).

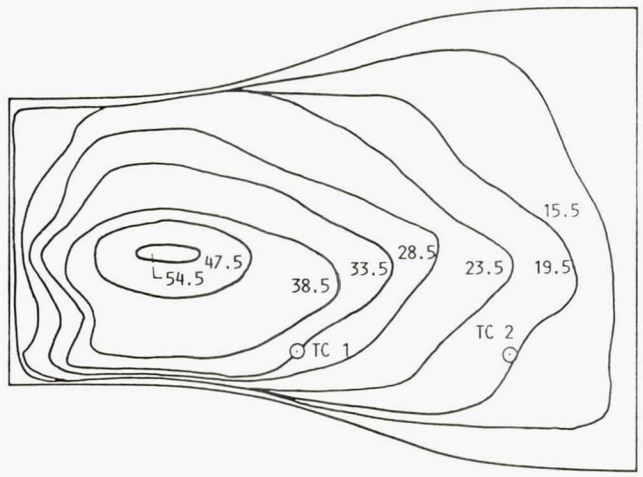

(b) Lower temperature liquid crystal (yellow = 35.6 °C).

Figure 22.—Yellow-color line positions shown as a function of time (seconds).

Concluding Remarks

Several flow visualization methods have been discussed along with some typical examples of their use. These experiments provided insight into the complex flow patterns which occur in aircraft engines, particularly around turbine passages. Some of the experiments also yielded quantitative information. This offers strong potential for use in validating analytical computer codes of fluid flow.

The use of liquid crystals for heat transfer studies was also described along with some typical results. These results gave both visual and quantitative information about heat transfer in turbine vane and blade passages. Although these experiments were directed toward the study of flow and heat transfer in aircraft turbines, the methods have potential application to a wide variety of scientific and technical disciplines.

References

1. Hah, C.; and Selva, R.J.: A Navier-Stokes Analysis of Flow and Heat Transfer Inside High-Pressure-Ratio Turbine Blade Rows. AIAA Paper 90-0343, Jan. 1990.
2. Simoneau, R.J.: Heat Transfer in Aeropropulsion Systems. Heat Transfer in High Technology and Power Engineering; Proceedings of the Joint Heat Transfer Seminar cosponsored by the National Science Foundation and Japan Society for the Promotion of Science, San Diego, California, September 17–20, 1985, W.-J. Yang and Y. Morie, eds., Hemisphere Publishing Corp., New York, 1987, pp. 285–319.
3. Liebert, C.H.; and Miller, R.A.: Ceramic Thermal Barrier Coatings. I & EC Product Research and Development, American Chemical Society, Sept. 1984, pp. 344–349.
4. Hale, P.W., et al.: Development of an Intergrated System for Flow Visualization in Air Using Neutrally-Buoyant Bubbles. SA1-RR-7107, Sage Action Inc., 1971.
5. Colladay, R.S.; and Russell, L.M.: Streakline Flow Visualization of Discrete-Hole Film Cooling with Normal, Slanted and Compound Angle Injection. NASA TN D-8248, 1976.
6. Gaugler, R.E.; and Russell, L.M.: Flow Visualization Study of the Horseshoe Vortex in a Turbine Stator Cascade. NASA TP-1884, 1982.
7. Russell, L.M.: Flow Visualization of Discrete-Hole Film Cooling With Spanwise Injection Over a Cylinder. NASA TP-1491, 1979.
8. Florschuetz, L.W., et al.: Multiple Jet Impingement Heat Transfer Characteristics: Experimental Investigation of In Line and Staggered Arrays With Crossflow. NASA CR-3217, 1980.
9. Langston, L.S.; and Boyle, M.T.: A New Surface Streamline Flow-Visualization Technique. J. Fluid Mech., vol. 125, Dec. 1982, pp. 53–57.
10. Braun, M.J., et al.: A Laser Based Computer Aided, Non-Intrusive Technique For Full Field Flow Characterization in Macroscopic Curved Channels. Flow Visualization—1989; Proceedings of the Symposium, ACME Winter Annual Meeting, San Francisco, CA., Dec. 10–15, 1989, B. Khalighi, M.J. Braun, and C.J. Freitas, eds., ACME, New York, 1989, pp. 15–22.
11. Hippensteele, S.A.; Russell, L.M.; and Stepka, F.S.: Evaluation of a Method for Heat Transfer Measurements and Thermal Visualization Using a Composite of a Heater Element and Liquid Crystals. NASA TM-81639, 1981.
12. Hippensteele, S.A.; Russell, L.M.; and Torres, F.J.: Local Heat Transfer Measurements on a Large Scale-Model Turbine Blade Airfoil Using a Composite of a Heater Element and Liquid Crystals. NASA TM-86900, 1985.
13. Hippensteele, S.A.; and Russell, L.M.: High-Resolution Liquid-Crystal Heat Transfer Measurements on the End Wall of a Turbine Passage with Variations in Reynolds Number. NASA TM-100827, 1988.
14. Jones, T.V.; and Hippensteele, S.A.: High-Resolution Heat-Transfer-Coefficient Maps Applicable to Compound-Curve Surfaces Using Liquid Crystals in a Transient Wind Tunnel. NASA TM-89855, 1988.

NASA
National Aeronautics and Space Administration

Report Documentation Page

1. Report No.	2. Government Accession No.	3. Recipient's Catalog No.
NASA TM-4272		

4. Title and Subtitle	5. Report Date
Visualization Techniques to Experimentally Model Flow and Heat Transfer in Turbine and Aircraft Flow Passages	June 1991
	6. Performing Organization Code

7. Author(s)	8. Performing Organization Report No.
Louis M. Russell and Steven A. Hippensteele	E-5811
	10. Work Unit No. 505-62-52

9. Performing Organization Name and Address	11. Contract or Grant No.
National Aeronautics and Space Administration Lewis Research Center Cleveland, Ohio 44135-3191	
	13. Type of Report and Period Covered: Technical Memorandum

12. Sponsoring Agency Name and Address	14. Sponsoring Agency Code
National Aeronautics and Space Administration Washington, D.C. 20546-0001	

15. Supplementary Notes

16. Abstract

Increased attention to fuel economy and increased thrust requirements have increased the demand for higher aircraft gas turbine engine efficiency through the use of higher turbine inlet temperatures. These higher temperatures increase the importance of understanding the heat transfer patterns which occur throughout the turbine passages. It is often necessary to use a special coating or some form of cooling to maintain metal temperatures at a level which the metal can withstand for long periods of time. Effective cooling schemes can result in significant fuel savings through higher allowable turbine inlet temperatures and can increase engine life. Before proceeding with the development of any new turbine it is economically desirable to create both mathematical and experimental models to study and predict flow characteristics and temperature distributions. This report describes some of the methods used to physically model heat transfer patterns, cooling schemes, and other complex flow patterns associated with turbine and aircraft passages.

17. Key Words (Suggested by Author(s))	18. Distribution Statement
Flow visualization Experimental heat transfer Turbines	Unclassified - Unlimited Subject Categories 34, 07

19. Security Classif. (of the report)	20. Security Classif. (of this page)	21. No. of pages	22. Price*
Unclassified	Unclassified	16	A03

NASA FORM 1626 OCT 86

*For sale by the National Technical Information Service, Springfield, Virginia 22161